

Exceptional points treatment of cavity spectroscopies

Shaul Mukamel

Department of Chemistry, University of California Irvine, Irvine, CA 92697, USA

Anqi Li and Michael Galperin*

Department of Chemistry & Biochemistry, University of California San Diego, La Jolla, CA 92093, USA

The infrared response of a system of two vibrational modes in a cavity is calculated by an effective non-Hermitian Hamiltonian derived by employing the nonequilibrium Green's functions (NEGF) formalism. Degeneracies of the Hamiltonian (exceptional points, EP) widely employed in theoretical analysis of optical cavity spectroscopies are used in an approximate treatment and compared with the full NEGF. Qualitative limitations of the EP treatment are explained by examining the approximations employed in the calculation.

I. INTRODUCTION

Developments in experimental techniques allow the spectroscopic measurements of molecular systems placed in cavities [1–11]. Cavity confinement promotes strong coupling between radiation field and molecular degrees of freedom. The optical control of molecular responses (conformational switching, charge and energy transfer, chemical reactions rates) thus becomes feasible. To enhance the signal, the majority of such experiments are performed on samples containing many molecules. However, spectroscopic measurements of single-molecules in plasmonic nanocavities were reported as well [12, 13].

Theoretical considerations of spectroscopy of molecules placed in optical cavities usually rely on simplified model approaches. While the actual experimental setup deals with open driven quantum mechanical systems, the simplest theoretical treatments use Hermitian Hamiltonian for the cavity mode and molecular degrees of freedom [14]. The open character of the system is introduced later in an ad hoc manner either using single particle scattering theory or within the input-output methodology, to name the two most popular and closely related approaches [15, 16]. In such treatments one diagonalizes the Hamiltonian matrix represented in a basis of isolated molecule many-body states with direct product with harmonic oscillator states representing the cavity mode. Its eigenstates mix different degrees of freedom of the system. The mixture of light and matter degrees of freedom are called polaritons.

More advanced treatments take into account the open character of the system already at the level of the Hamiltonian formulation - an effective non-Hermitian Hamiltonian consideration. Non-Hermitian quantum mechanics is implemented in many research areas from optics, to quantum field theory, to molecular physics [17, 18]. Non-Hermitian quantum mechanics is obtained by adding complex absorbing potentials (CAPs) to Hermitian Hamiltonians. CAPs which represent the open

character of the system are often employed to simplify numerical simulations. System responses are especially non-trivial at the degeneracy points of the non-Hermitian Hamiltonian spectrum known as exceptional points (EPs) [19–21]. The concept is widely applied in the description of open quantum systems [22, 23] including studies of quantum transport at junctions [24, 25]. It is also popular in optics and polaritonics [26–31] where EPs were shown to be responsible for exotic phenomena such as decreasing intensity of the emitted laser light for increasing pump power [32], unidirectional transport [33], chiral modes [34, 35], and anomalous lasing [36, 37]. In addition, topological structures [38–41], phase transitions [42, 43], and topological Berry phase [44, 45] are observed in the vicinity of exceptional points.

First principles treatment of open quantum systems starts with a Hermitian quantum mechanical description of the universe. Description of the open system is obtained by tracing out environmental (bath) degrees of freedom. The nonequilibrium Green's function (NEGF) approach to open quantum systems follows this paradigm [46, 47]. The influence of environment is then incorporated through the self-energies.

Here, we study a model of two vibrational modes in a cavity. The vibrations are not directly coupled but are coupled to the cavity mode and to thermal (phonon) baths. The cavity mode is driven by laser modeled as a continuum of radiation modes narrowly populated around the laser frequency. The model was discussed previously within the non-Hermitian quantum mechanics paradigm where effective non-Hermitian Hamiltonian derived within the input-output formalism consideration was used for consideration of the role of exceptional points in responses of the open quantum system [48]. Here we adopt a non-Hermitian quantum mechanics formulation starting with the exact NEGF description. We then discuss concept of exceptional points and compare the predictions of the non-Hermitian simulations to those of the more rigorous full NEGF results.

The structure of the paper is as follows. In Section II we introduce the model, present corresponding NEGF formulation, and use it to derive non-Hermitian quantum mechanical description. Section III presents numerical

* migalperin@ucsd.edu

simulations performed within NEGF and within exceptional points approaches and discusses similarities and differences of the two methods. Conclusions are drawn in Section IV.

II. TWO VIBRATIONAL MODES IN A CAVITY

A. Model

We consider two vibrational modes ω_1 and ω_2 coupled to the same cavity mode ω_C and driven by the same laser field (see Fig. 1). The vibrational modes are coupled further to thermal baths. In the rotating wave approximation the Hamiltonian of the system is

$$\hat{H} = \hat{H}_0 + \hat{V} \quad (1)$$

where

$$\begin{aligned} \hat{H}_0 &= \omega_C \hat{a}_C^\dagger \hat{a}_C + \sum_{i=1,2} \omega_i \hat{b}_i^\dagger \hat{b}_i \\ &+ \sum_{\alpha} \omega_{\alpha} \hat{a}_{\alpha}^\dagger \hat{a}_{\alpha} + \sum_{i=1,2} \sum_{\beta_i} \omega_{\beta_i} \hat{b}_{\beta_i}^\dagger \hat{b}_{\beta_i} \\ \hat{V} &= \sum_i g_i \hat{a}_C^\dagger \hat{a}_C (\hat{b}_i + \hat{b}_i^\dagger) \\ &+ \sum_{\alpha} (V_{C\alpha} \hat{a}_C^\dagger \hat{a}_{\alpha} + V_{\alpha C} \hat{a}_{\alpha}^\dagger \hat{a}_C) \\ &+ \sum_{i=1,2} \sum_{\beta_i} (V_{i\beta_i} \hat{b}_i^\dagger \hat{b}_{\beta_i} + V_{\beta_i i} \hat{b}_{\beta_i}^\dagger \hat{b}_i) \end{aligned} \quad (2)$$

Here, the boson operators \hat{a}_C^\dagger and \hat{b}_i^\dagger create quanta of cavity mode excitation and vibration i , respectively. \hat{a}_{α}^\dagger and $\hat{b}_{\beta_i}^\dagger$ describe excitations of radiation field and phonon (thermal) baths, respectively.

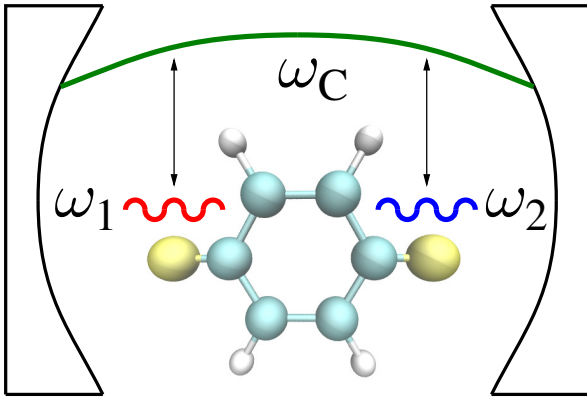


FIG. 1. Sketch of a single molecule in a cavity model.

B. The NEGF formulation

We first consider the cavity mode and vibrations by ignoring mixing between the cavity mode and vibrational degrees of freedom. The corresponding single-particle Green's functions are defined on the Keldysh contour as

$$\begin{aligned} A_C(\tau_1, \tau_2) &\equiv -i \langle T_c \hat{a}_C(\tau_1) \hat{a}_C^\dagger(\tau_2) \rangle \\ B_{ij}(\tau_1, \tau_2) &\equiv -i \langle T_c \hat{b}_i(\tau_1) \hat{b}_j^\dagger(\tau_2) \rangle \quad (i, j = 1, 2) \end{aligned} \quad (3)$$

Here, $\tau_{1,2}$ are contour variables and T_c is the contour ordering operator. These Green's functions satisfy the Dyson equations

$$\begin{aligned} \left(i \frac{\partial}{\partial \tau_1} - \omega_C \right) A_C(\tau_1, \tau_2) &= \delta(\tau_1, \tau_2) \\ &+ \int_c d\tau \Sigma_A(\tau_1, \tau) A_C(\tau, \tau_2) \\ \left(i \frac{\partial}{\partial \tau_1} \mathbf{I} - \mathbf{\Omega} \right) \mathbf{B}(\tau_1, \tau_2) &= \delta(\tau_1, \tau_2) \mathbf{I} \\ &+ \int_c d\tau \mathbf{\Sigma}_B(\tau_1, \tau) \mathbf{B}(\tau, \tau_2) \end{aligned} \quad (4)$$

where \mathbf{I} is unity matrix,

$$\mathbf{\Omega} = \begin{pmatrix} \omega_1 & 0 \\ 0 & \omega_2 \end{pmatrix}, \quad (5)$$

and

$$\begin{aligned} \Sigma_A(\tau_1, \tau_2) &= \Sigma_{rad}(\tau_1, \tau_2) + \Sigma_{vib}(\tau_1, \tau_2) \\ \Sigma_B(\tau_1, \tau_2) &= \Sigma_{ph}(\tau_1, \tau_2) + \Sigma_C(\tau_1, \tau_2) \end{aligned} \quad (6)$$

are self-energies. The latter account for effect of couplings to the radiation field and phonon baths,

$$\begin{aligned} \Sigma_{rad}(\tau_1, \tau_2) &= \sum_{\alpha} V_{C\alpha} A_{\alpha}(\tau_1, \tau_2) V_{\alpha C} \\ [\Sigma_{ph}]_{ii}(\tau_1, \tau_2) &= \sum_{\beta_i} V_{i\beta_i} B_{\beta_i}(\tau_1, \tau_2) V_{\beta_i i} \end{aligned} \quad (7)$$

and for interaction between the cavity mode and vibrational degrees of freedom. In the second order diagrammatic expansion the latter are

$$\begin{aligned} \Sigma_{vib}(\tau_1, \tau_2) &= i \sum_{i,j} g_i \left(B_{ij}(\tau_1, \tau_2) + B_{ij}(\tau_2, \tau_1) \right) g_j \\ [\Sigma_C]_{ij}(\tau_1, \tau_2) &= i g_i P(\tau_1, \tau_2) g_j \end{aligned} \quad (8)$$

$A_{\alpha}(\tau_1, \tau_2)$ and $B_{\beta_i}(\tau_1, \tau_2)$ are respectively the Green's function of free photons and phonons,

$$\begin{aligned} A_{\alpha}(\tau_1, \tau_2) &\equiv -i \langle T_c \hat{a}_{\alpha}(\tau_1) \hat{a}_{\alpha}^\dagger(\tau_2) \rangle_0 \\ B_{\beta_i}(\tau_1, \tau_2) &\equiv -i \langle T_c \hat{b}_{\beta_i}(\tau_1) \hat{b}_{\beta_i}^\dagger(\tau_2) \rangle_0, \end{aligned} \quad (9)$$

and

$$P(\tau_1, \tau_2) \equiv -\langle T_c \hat{a}_C^\dagger(\tau_1) \hat{a}_C(\tau_1) \hat{a}_C^\dagger(\tau_2) \hat{a}_C(\tau_2) \rangle \quad (10)$$

is the polarization bubble (two-particle Green's function of the cavity mode excitations).

To compute the Green's functions (3) one has to solve the system of coupled Dyson equations (4) self-consistently on the Keldysh contour. Because the self-energy Σ_c in Eq. (8) is expressed in terms of two-particle Green's function (10) simultaneous solution of the Bethe-Salpeter equation should be considered for the polarization bubble. To simplify the analysis we neglect effect of vibrational degrees of freedom on cavity mode. In this case the self-energy $\Sigma_{vib}(\tau_1, \tau_2)$ in Eq.(8) can be dropped and the polarization bubble (10) can be approximately expressed in terms of single-particle Green's functions A_C using the Wick's theorem

$$[\Sigma_C]_{ij}(\tau_1, \tau_2) \approx i g_i A_C(\tau_1, \tau_2) A_C(\tau_2, \tau_1) g_j \quad (11)$$

C. Linearization of the polarization bubble

After neglecting back action of vibrational degrees of freedom on cavity mode, assuming wide band approximation for coupling to radiation field modes, considering steady-state, and taking Fourier transform we get from (6) for retarded and lesser projections of Σ_A

$$\begin{aligned} \Sigma_A^r(E) &= -\frac{i}{2}\kappa \\ \Sigma_A^<(E) &= -i\kappa \frac{P}{\omega_L} \frac{\delta}{(E - \omega_L)^2 + (\delta/2)^2} \end{aligned} \quad (12)$$

Here, κ is cavity mode dissipation, ω_L is the laser frequency, δ is the laser linewidth, and P is the laser intensity. Thus,

$$\begin{aligned} \langle \hat{a}_C^\dagger \hat{a}_C \rangle &= i A_C^<(t, t) \\ &= i \int \frac{dE}{2\pi} A_C^r(E) \Sigma_A^<(E) A_C^a(E) \\ &\xrightarrow{\delta \rightarrow 0^+} \kappa \frac{P}{\omega_L} A_C^r(\omega_L) A_C^a(\omega_L) \end{aligned} \quad (13)$$

We split the total cavity field into the pumped field α_c (treated classically) and and fluctuations $\delta\hat{a}_c$ due to presence of empty radiation background (treated quantum mechanically)

$$\hat{a}_C = \alpha_C + \delta\hat{a}_C \quad (14)$$

Thus,

$$\begin{aligned} \langle \hat{a}_C^\dagger \hat{a}_C \rangle &= \alpha_C^* \alpha_C \Rightarrow \\ \alpha_C &= \sqrt{\kappa \frac{P}{\omega_L}} \frac{1}{\omega_L - \omega_C + \frac{i}{2}\kappa} \equiv \epsilon \frac{1}{\Delta + \frac{i}{2}\kappa} \end{aligned} \quad (15)$$

where $\epsilon \equiv \sqrt{\kappa P/\omega_L}$ is the driving strength and $\Delta \equiv \omega_L - \omega_C$ is the detuning between the pumping laser field and cavity mode frequency.

Linearization of the polarization bubble (10) yields

$$\begin{aligned} P(\tau_1, \tau_2) &= -\left\langle T_c \left(\alpha_C^* + \delta a_C^\dagger(\tau_1) \right) (\alpha_C + \delta \hat{a}_C(\tau_1)) \right. \\ &\quad \left. \times \left(\alpha_C^* + \delta a_C^\dagger(\tau_2) \right) (\alpha_C + \delta \hat{a}_C(\tau_2)) \right\rangle \\ &\approx -i \alpha_C^* \alpha_C \left(\mathcal{A}_C(\tau_1, \tau_2) + \mathcal{A}_C(\tau_2, \tau_1) \right) \end{aligned} \quad (16)$$

where

$$\mathcal{A}_C(\tau, \tau') \equiv -i \langle T_c \delta \hat{a}_C(\tau) \delta \hat{a}_C^\dagger(\tau') \rangle \quad (17)$$

is the single-particle Green's function of cavity mode fluctuations coupled to an empty continuum of radiation field modes. Green's function (17) satisfies the Dyson equation

$$\begin{aligned} \left(i \frac{\partial}{\partial \tau_1} + \Delta \right) \mathcal{A}_C(\tau_1, \tau_2) &= \delta(\tau_1, \tau_2) \\ &+ \int_c d\tau \Sigma_{rad}^{empty}(\tau_1, \tau) \mathcal{A}_C(\tau, \tau_2) \end{aligned} \quad (18)$$

Separation of the field into two parts with one, α_C , treated classically and the other, $\delta\hat{a}_C$, quantum mechanically introduces several approximations:

1. The main difference between classical and quantum fields is the ability of the latter to mediate photon supported effective interaction between quantum degrees of freedom in the system. For the model considered here, quantum degrees of freedom interacting via photon are molecular vibrations, and photon induced interaction is described by Σ_C . Expressions for the interaction, Eq.(11) for NEGF and Eq.(23) below for EP, become very different in strong fields, where neglected quantum character of the α_C part becomes pronounced.
2. A classical treatment misses all quantum correlations. This is reflected by time-local character of α_C contribution vs. time-non-local correlation functions in quantum treatment.
3. α_C and $\delta\hat{a}_C$ of Eq.(14) are two parts representing the same radiation field mode. Thus, in the case of spontaneous emission, described within the $\delta\hat{a}_C$ part, resulting photon should be accounted for in the α_C part. In the linearized formulation such photon is disregarded. The effect should be significant at weak laser fields.

This completes the description of the cavity mode. Below we focus on dynamics of the vibrational degrees of freedom. The result for the linearized polarization bubble P , Eq.(16), can now be used in expression for self-energy of vibrations due to coupling to the cavity mode Σ_C , Eq.(8)

D. Exceptional points

To introduce the concept of exceptional points one has to formulate the dynamics of the two vibrational degrees of freedom in terms of some effective non-Hermitian Hamiltonian \hat{H}_{eff} . Within the NEGF (assuming steady-state) this is equivalent to substituting proper on-the-contour Dyson equation for the Green's function \mathbf{B} ,

$$\begin{bmatrix} E\mathbf{I} - \mathbf{\Omega} - \mathbf{\Sigma}_B^c(E) & \mathbf{\Sigma}_B^<(E) \\ \mathbf{\Sigma}_B^>(E) & -E\mathbf{I} + \mathbf{\Omega} - \mathbf{\Sigma}_B^{\tilde{c}}(E) \end{bmatrix} \times \begin{bmatrix} \mathbf{B}^c(E) & \mathbf{B}^<(E) \\ \mathbf{B}^>(E) & \mathbf{B}^{\tilde{c}}(E) \end{bmatrix} = \mathbf{I}, \quad (19)$$

with an effective equation-of-motion,

$$\begin{bmatrix} E\mathbf{I} - \mathbf{H}_{eff} & 0 \\ 0 & -E\mathbf{I} + \mathbf{H}_{eff} \end{bmatrix} \begin{bmatrix} \mathbf{B}^c(E) & \mathbf{B}^<(E) \\ \mathbf{B}^>(E) & \mathbf{B}^{\tilde{c}}(E) \end{bmatrix} = \mathbf{I}, \quad (20)$$

Here, c , $<$, $>$, and \tilde{c} indicate causal, lesser, greater, and anti-causal projections, respectively. Taking into account that

$$\begin{aligned} \mathbf{\Sigma}_B^c(E) &= \mathbf{\Sigma}_B^r(E) + \mathbf{\Sigma}_B^<(E) \\ \mathbf{\Sigma}_B^{\tilde{c}}(E) &= \mathbf{\Sigma}_B^a(E) + \mathbf{\Sigma}_B^>(E) \end{aligned} \quad (21)$$

(here r and a are retarded and advanced projections) transition from (19) to (20) is only meaningful under the following assumptions:

1. Lesser projection of the self-energy is disregarded

$$\mathbf{\Sigma}_B^<(E) \equiv \mathbf{\Sigma}_{ph}^<(E) + \mathbf{\Sigma}_C^<(E) = 0$$

- (a) Thermal (phonon) bath contribution can be disregarded when the bath is held at zero temperature, that is $\mathbf{\Sigma}_{ph}^<(E) = 0$.

- (b) Neglecting contribution $\mathbf{\Sigma}_C^<(E)$ is consistent with the assumption of the field splitting, so that $\langle \delta \hat{a}_C^\dagger \delta \hat{a}_C \rangle = 0$, but requires also assuming $\langle \delta \hat{a}_C \delta \hat{a}_C^\dagger \rangle = 0$ (i.e. neglect quantum character of the radiation background) which is hard to justify.

2. Greater projection of the self-energy is disregarded

$$\mathbf{\Sigma}_B^>(E) \equiv \mathbf{\Sigma}_{ph}^>(E) + \mathbf{\Sigma}_C^>(E) = 0$$

This assumption is equivalent to neglect of quantum effects in the bath which contradicts zero temperature requirement of the previous step. Indeed, considering lesser and greater projections of phonon self-energy Σ_{ph} : $\Sigma_{ph}^<(E) = -i\gamma(E)N(E)$ and $\Sigma_{ph}^>(E) = -i\gamma(E)[1 + N(E)]$ (here, $\gamma(E)$ the dissipation rate and $N(E)$ is the Bose-Einstein phonon distribution in thermal bath) one sees that when $T \rightarrow 0 \Rightarrow N(E) \rightarrow 0$. This justifies neglect of the lesser projection. However, quantum effects in principle do not allow similar neglect of the greater projection of the self-energy: $\Sigma_{ph}^E \xrightarrow{T \rightarrow 0} -i\gamma(E)$.

3. On the scale of the system relevant energies energy dependence of the self-energy projections is smooth, so that

$$\mathbf{\Sigma}_B^{r/a}(E) \approx \mathbf{\Sigma}_B^{r/a}(E_0) = \text{const}$$

for some arbitrary energy E_0 .

To obtain an effective vibrational Hamiltonian we only need to know the retarded projection of the self-energy $\mathbf{\Sigma}_B$, which according to Eq.(6) has contributions from coupling to thermal bath, $\mathbf{\Sigma}_{ph}^r$, and interaction via cavity mode, $\mathbf{\Sigma}_C^r$. Neglecting bath induced correlations and assuming wide band approximation (WBA) the former is

$$\mathbf{\Sigma}_{ph}^r(E) = -\frac{i}{2} \begin{bmatrix} \gamma_1 & 0 \\ 0 & \gamma_2 \end{bmatrix} \quad (22)$$

Here $\gamma_i(E) \equiv 2\pi \sum_{\beta_i} V_{i\beta_i} V_{\beta_i i} \delta(E - \omega_{\beta_i})$ ($i = 1, 2$) is the dissipation rate of vibrational mode i . The latter is obtained using (16) and (18) in (8)

$$\begin{aligned} \mathbf{\Sigma}_C^r(E) &= g_i \alpha_C^* \alpha_C g_j \left(\mathcal{A}_C^r(E) + \mathcal{A}_C^a(-E) \right) \\ &= g_i \alpha_C^* \alpha_C g_j \left(\frac{1}{\Delta + E + \frac{i}{2}\kappa} + \frac{1}{\Delta - E - \frac{i}{2}\kappa} \right) \end{aligned} \quad (23)$$

Finally, utilizing (15), taking $g_1 = g_2 \equiv g$, choosing an arbitrary value E_0 in (23), and adding (22) yields effective Hamiltonian

$$\mathbf{H}_{eff} = \begin{bmatrix} \omega_1 - \frac{i}{2}\gamma_1 + \Lambda & \Lambda \\ \Lambda & \omega_2 - \frac{i}{2}\gamma_2 + \Lambda \end{bmatrix} \quad (24)$$

where

$$\begin{aligned} \Lambda &\equiv g^2 \frac{P}{\omega_L} \frac{\kappa}{\Delta^2 + \frac{\kappa^2}{4}} \\ &\times \left[\frac{\Delta + E_0 - \frac{i}{2}\kappa}{(\Delta + E_0)^2 + \frac{\kappa^2}{4}} + \frac{\Delta - E_0 + \frac{i}{2}\kappa}{(\Delta - E_0)^2 + \frac{\kappa^2}{4}} \right] \end{aligned} \quad (25)$$

The eigenenergies of the Hamiltonian are

$$\begin{aligned} E_{\pm} &= \frac{\omega_1 - \frac{i}{2}\gamma_1 + \Lambda + \omega_2 - \frac{i}{2}\gamma_2 + \Lambda}{2} \\ &\pm \frac{1}{2} \sqrt{\left[\left(\omega_1 - \frac{i}{2}\gamma_1 \right) - \left(\omega_2 - \frac{i}{2}\gamma_2 \right) \right]^2 + 4\Lambda^2} \end{aligned} \quad (26)$$

Thus, exceptional point (defined as point of degeneracy for eigenvalues) is

$$\left[\left(\omega_1 - \frac{i}{2}\gamma_1 \right) - \left(\omega_2 - \frac{i}{2}\gamma_2 \right) \right]^2 + 4\Lambda^2 = 0 \quad (27)$$

These results were first obtained in Ref. [48] using the input-output formalism.

To re-introduce information on the baths, the input-output formalism utilizes concept of noise operators.

Their correlation functions yield lesser and greater projections of the corresponding self-energies, $\Sigma_{rad}^{\lessgtr}(E)$ and $\Sigma_{ph}^{\lessgtr}(E)$, usually taken at a particular fixed energy E_0 (delta-correlated in time). In this respect, the input-output formalism is similar to the single-particle scattering theory. Note that lesser and greater projections of the self-energy due to coupling between vibrational and cavity modes, $\Sigma_C^{\lessgtr}(E)$, are not taken into account by the procedure and thus are disregarded in the EP treatment. Strictly speaking such consideration is inconsistent, because retarded projection of the same self-energy, $\Sigma_C^r(E)$, plays central role in the EP approach. The three projections are not independent, all three are related to the same self-energy defined on the Keldysh contour. Thus, keeping one of the projections while ignoring the others is inconsistent. In terms of physical effects, retarded projection yields information on the level shift and dissipation, while lesser and greater projections describe ability to in- and out-scattering of energy quanta. Ignoring the latter while keeping the former is equivalent to neglect of energy exchange between molecular degrees of freedom. Also, it leads to violation of the fluctuation-dissipation relations. Thus, besides disregarding energy transfer between molecular vibrations due to radiation field-induced interaction, such description will not allow to reach correct thermal equilibrium.

Knowledge of the B Green's functions, Eq.(3), within the NEGF formalism or effective Hamiltonian \hat{H}^{eff} , Eq.(24), within the EP formalism allows to simulate multiple system characteristics (energy flux, populations of the modes, spectrum, effective temperatures, etc.). Below, following Ref. [48] we focus on simulation of the spectra of vibrational degrees of freedom and their effective temperatures.

III. NUMERICAL RESULTS

While the EP approach is widely applied in optomechanics [41, 48–51] its applicability in single-molecule cavity systems [12, 13] is not well established. Here, we compare calculations obtained utilizing exceptional points (EP) with those of the full NEGF simulations for a single-molecule in a cavity at steady-state regime.

Following Ref. [48] we focus on simulation of the spectra of vibrational degrees of freedom and of their effective temperatures. The former is defined by lesser projection of the Green function B . At steady state,

$$S_i(E) \equiv i B_{ii}^<(E) \quad (i = 1, 2) \quad (28)$$

Usually exceptional points indicate thresholds for significant changes in the system response. In particular, for our model only one EP (27) is possible. It was shown in Ref. [48] that this exceptional point yields a critical value of effective inter-mode coupling Λ . Coupling strengths below the critical value provide spectrum with peaks at

the vibrational mode frequencies. Couplings above the critical value yield splitting in the spectrum.

Effective temperature is obtained from assumption of the thermal vibrational distribution

$$k_B T_i^{eff} \equiv \frac{\hbar \omega_i}{\log \left(1 + \left[\int \frac{dE}{2\pi} S_i(E) \right]^{-1} \right)} \quad (29)$$

In derivation of Eq.(29) we use the Bose-Einstein distribution instead of its limiting value $k_B T_i^{eff}/\hbar \omega_i$ used in Ref. [48] which does not apply for our choice of parameters.

We perform the simulations using typical parameters for a single molecule in a cavity setup: cavity mode with frequency $\omega_C = 2$ eV and escape rate $\kappa = 10^{-3}$ eV is pumped with a monochromatic laser with frequency $\omega_L = 1.5$ eV and linewidth $\delta = 10^{-5}$ eV. Molecular vibrations $\omega_1 = 0.1$ eV and $\omega_2 = 0.08$ eV are coupled two different thermal baths. Energy escape rates to the baths are $\gamma_1 = 10^{-3}$ eV and $\gamma_2 = 5 \times 10^{-4}$ eV. Coupling strengths of the vibrations to the cavity mode are $g_1 = g_2 = 0.05$ eV. Realistic laser intensities used in optical experiments with single molecule junctions are ~ 1 kW/cm² [52]. This together with characteristics cross-section of 3 nm² and laser frequency $\omega_L = 1.5$ eV ($\lambda_L \sim 780$ nm) yields $P/\omega_L \sim 10^4$ eV.

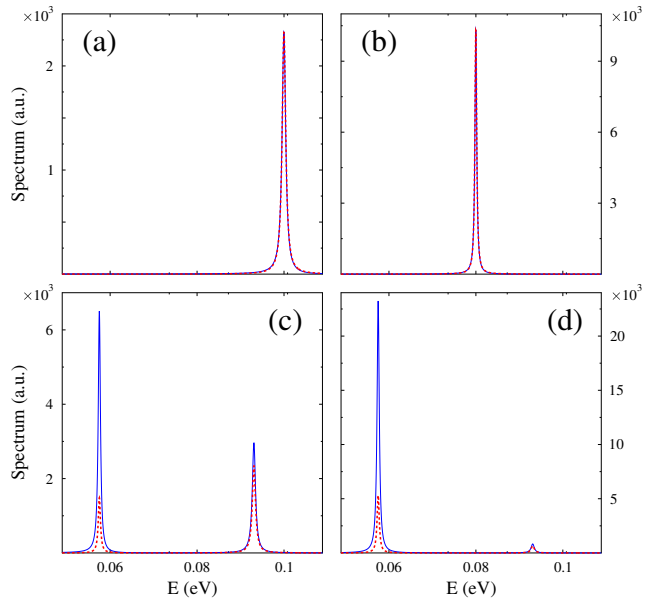


FIG. 2. Vibrational spectrum $S(E)$, Eq.(28), in a cavity. Shown are results of calculations within EP (dashed line, red) and NEGF (solid line, blue) approaches for ω_1 with inter-mode coupling (a) below and (c) above exceptional point value. Similar results for ω_2 are shown in panels (b) and (d), respectively. See text for parameters.

For the chosen parameters the critical value of inter-mode coupling, Eq.(27), is $\Lambda \sim 0.01$ eV which correspond to $P/\omega_L \sim 10^2$ eV. Figure 2 shows the infrared

vibrational spectrum, Eq.(28), for effective coupling Λ below (top row, $P/\omega_L = 10$ eV) and above (bottom row, $P/\omega_L = 10^4$ eV) its critical value. As expected, the spectrum shows mode splitting for values of the coupling above the exceptional point, Eq.(27). For the chosen parameters EP and NEGF yield similar results for $P/\omega_L = 10$ eV, the differences appear at strong couplings: results for heights of peaks in the spectrum (including qualitative relative peak values) are predicted differently by the two approaches. An obvious reason for the discrepancy is neglect of self-energy $\Sigma_C^<$ in the EP formulation which becomes pronounced for stronger couplings. Disregarding $\Sigma_C^<$ leads to the neglect of energy exchange between molecular vibrations and violates fluctuation-dissipation relations. One sees that for the particular choice of parameters discrepancy in prediction of position and width of peaks is relatively small. This is expected because retarded projection of self-energy Σ_B , Eq.(6), to which Σ_C^r contributes is responsible for peaks shifts (real part of Σ_B^r) and widths (imaginary part of Σ_B^r). Note however that by its very construction the EP approach disregards self-consistency of the complete NEGF treatment (see discussion in the conclusions). This lack of self-consistency results in incorrect Σ_C^r contribution. Note also that because the EP misses quantum correlations between vibrations (consequence of the linearization procedure), another choice of parameters may lead to different results for the two approaches also for small values of inter-mode coupling.

While low power results coincide for the parameters chosen, we note that this cannot be considered as validation of the EP approach. Close or coinciding results at a particular set of parameters in principle cannot be a proof of quality of a theory. This is no more than an illustration that for the particular set of parameters inherent (built in) mistakes of the EP theory are numerically small. However, it does not make the EP approach a consistent theory. In terms of physics, the disregarded lesser and greater projections of self-energy Σ_C are responsible for energy exchange between molecular vibrations caused by cavity mode induced effective interaction. Among other parameters, intensity of radiation field defines strength of the exchange. Indeed, intensity of radiation field enters $\Sigma_C^>$ via greater/lesser projections of Green function A , Eq.(11), which in turn is defined by $\Sigma_A^>$, Eq.(6), whose Σ_{rad} contribution, Eq.(7), is directly proportional to the field intensity. Thus, it is not surprising that at low intensities the mistake of the EP approach is less pronounced numerically.

Figure 3 shows the effective temperatures of the modes, Eq.(29), as functions of the laser intensity. Discrepancy between EP and NEGF in spectrum results naturally leads to quantitative and qualitative differences in predicting temperatures of the modes. For example, Fig. 3a shows that the EP approach predicts cooling of the mode ω_2 when increasing laser frequency, while proper NEGF simulation show the mode will be heated and its heating will be more significant than that of mode ω_1 . Similarly,

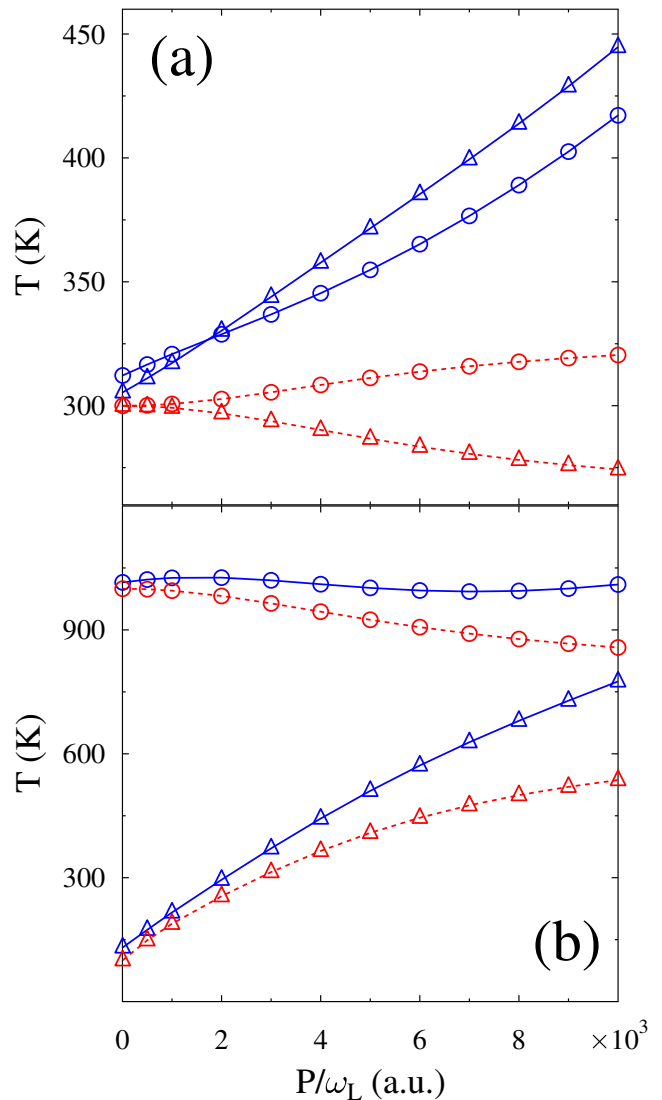


FIG. 3. Effective temperature T^{eff} , Eq.(29), vs the pump laser intensity. Shown are results of calculations within EP (dashed line, red) and NEGF (solid line, blue) approaches for ω_1 (circles) and ω_2 (triangles). Calculation are performed for (a) $T_1 = T_2 = 300$ K and (b) $T_1 = 1000$ K and $T_2 = 100$ K. Other parameters are as in Fig. 2.

Fig. 3b shows the EP prediction for monotonic cooling of T_1^{eff} , while NEGF yields non-monotonic behavior.

IV. CONCLUSIONS

Starting with the full NEGF treatment of two vibrations in a cavity (Fig. 1) we derive an effective non-Hermitian Hamiltonian formulation and discuss the employed approximations. The effective Hamiltonian allows to introduce exceptional points (degeneracy points in the spectrum of the Hamiltonian). Together with the input-output formalism the approach is widely used in the the-

oretical analysis of optomechanical systems.

The main limitations of the EP approach are related to

1. Its Markov (delta correlated in time) character, which makes it inconvenient in treatment of systems with multiple resonances.
2. Its inconsistency in treatment of intra-system interactions which results in keeping retarded projection of the corresponding self-energy while disregarding all other projections of the same self-energy.

For simplicity we disregarded the back action of vibrational modes. This was done intentionally because incorporation of self-consistency into the NEGF treatment would make derivation of the EP approach from NEGF impossible and thus distract from the main message of the paper. We note that strictly speaking accounting for back action within NEGF is not a matter of choice but a necessity. Ever since classical works by Kadanoff and Baym in 1960s [53, 54], it is known that non-self-consistent approximations within NEGF violate conservation laws in the system. While the limitation of bare perturbation theory is well known in quantum transport, optics community is less aware about the problem. This limitation was a focus of our previous studies [55, 56]. With the presented derivation we show that the EP approach is not capable to account for the self-consistency by its very construction. This is one more limitation of the EP method. From physics point of view necessity of self-consistent treatment is direct consequence of necessity to balance properly energy exchange between the two molecular vibrations. Steady-state situation results from multiple energy exchanges. While the effect is not expected to be very important due to the large difference in corresponding frequencies, in other systems (e.g. in quantum transport applications) inherent lack of self-consistency in the EP treatment may be one more source of mistake.

We compare the NEGF and EP predictions for parameters chosen to represent single-molecule in a cavity. EP is shown to miss important information which (for the chosen parameters) leads to qualitatively incorrect predictions of spectra and effective temperatures of the vibrational modes. Note that the discrepancy between NEGF and EP results is pronounced at strong laser fields, where quantum effects (missed by the EP approach) are not the main factor.

While our discussion was focused on optomechanics (as a convenient model to show limitations of the EP treatment) similar conclusions are relevant for standard po-

laritonic treatment: while number of peaks in polaritonic spectrum will be the same within the EP and a more rigorous treatments (3 in a similar polaritonic model), their positions, heights, and linewidths may differ significantly. Note that similar to situation with quantum transport where for non-interacting systems the full NEGF treatment can be substituted with much simpler scattering theory based (Landauer-Buttiker) approach, also in polaritonic systems with many molecules situation depends on level of the theory involved. If one considers a set of non-interacting molecules each individually coupled to cavity mode with mode-induced inter-molecular interaction disregarded (that is a non-interacting set of molecules), existing scattering theory based approaches will be capable to describe such a situation. However, the moment one is willing to introduce any sort of interaction into consideration (besides individual molecule mixing with radiation field mode resulting in polariton) with energy redistribution between the system degrees of freedom existing techniques will fail due to the same reasons as considered in the manuscript. Note also that the conclusions are equally applicable to any order of optical processes in nanocavity systems. Indeed, the very classification of spectroscopies (processes of particular order) accepted in optics community is not applicable to open systems. One can introduce a somewhat meaningful analog of such classification by separating the total photon flux into ‘different order’ contributions (please, note that such separation is not rigorous due to the same reasons why one cannot rigorously separate total electronic current into elastic and inelastic fluxes - see e.g. Ref. [57]). We discussed the issue in our previous publication [56]. However, such separation is a post-processing. That is, central object of study in NEGF is the total photon flux, which includes in it all contributions (optical processes of all orders).

In summary, a careful analysis of the involved approximations should be performed prior to employing the EP method (and concept of exceptional points) in treatment of nanoscale systems. In particular, for systems with several participating resonances, systems with significant redistribution of population between degrees of freedom (DOF) or with pronounced effect of back action between the DOFs EP formalism will not be accurate.

ACKNOWLEDGMENTS

This material is based upon work supported by the National Science Foundation under Grant No. CHE-2154323 (M.G.) and Grant No. CHE-2246379 (S.M.)

[1] T. Schwartz, J. A. Hutchison, C. Genet, and T. W. Ebbesen, *Phys. Rev. Lett.* **106**, 196405 (2011).
 [2] J. A. Hutchison, T. Schwartz, C. Genet, E. Devaux, and T. W. Ebbesen, *Angewandte Chemie International Edi-*

tion **51**, 1592 (2012).
 [3] J. A. Hutchison, A. Liscio, T. Schwartz, A. Canaguier-Durand, C. Genet, V. Palermo, P. Samorì, and T. W. Ebbesen, *Adv. Mater.* **25**, 2481 (2013).

- [4] T. Schwartz, J. A. Hutchison, J. Léonard, C. Genet, S. Haacke, and T. W. Ebbesen, *ChemPhysChem* **14**, 125 (2013).
- [5] A. W. Eddins, C. C. Beedle, D. N. Hendrickson, and J. R. Friedman, *Phys. Rev. Lett.* **112**, 120501 (2014).
- [6] E. Eizner, K. Akulov, T. Schwartz, and T. Ellenbogen, *Nano Lett.* **17**, 7675 (2017).
- [7] G. G. Rozenman, K. Akulov, A. Golombek, and T. Schwartz, *ACS Photonics* **5**, 105 (2018).
- [8] K. Akulov, D. Bochman, A. Golombek, and T. Schwartz, *J. Phys. Chem. C* **122**, 15853 (2018).
- [9] B. Xiang, R. F. Ribeiro, M. Du, L. Chen, Z. Yang, J. Wang, J. Yuen-Zhou, and W. Xiong, *Science* **368**, 665 (2020).
- [10] T.-T. Chen, M. Du, Z. Yang, J. Yuen-Zhou, and W. Xiong, *Science* **378**, 790 (2022).
- [11] Z. Yang and W. Xiong, *Advanced Quantum Technologies* **5**, 2100163 (2022), eprint: <https://onlinelibrary.wiley.com/doi/pdf/10.1002/qute.202100163>.
- [12] R. Chikkaraddy, B. de Nijs, F. Benz, S. J. Barrow, O. A. Scherman, E. Rosta, A. Demetriadou, P. Fox, O. Hess, and J. J. Baumberg, *Nature* **535**, 127 (2016).
- [13] F. Benz, M. K. Schmidt, A. Dreismann, R. Chikkaraddy, Y. Zhang, A. Demetriadou, C. Carnegie, H. Ohadi, B. de Nijs, R. Esteban, J. Aizpurua, and J. J. Baumberg, *Science* **354**, 726 (2016).
- [14] R. F. Ribeiro, A. D. Dunkelberger, B. Xiang, W. Xiong, B. S. Simpkins, J. C. Owrutsky, and J. Yuen-Zhou, *The Journal of Physical Chemistry Letters* **9**, 3766 (2018).
- [15] K. K. Lehmann and D. Romanini, *J. Chem. Phys.* **105**, 10263 (1996).
- [16] C. Ciuti and I. Carusotto, *Phys. Rev. A* **74**, 033811 (2006).
- [17] N. Moiseyev, *Non-Hermitian Quantum Mechanics* (Cambridge University Press, Cambridge, 2011).
- [18] S. R.-K. Rodriguez, *Eur. J. Phys.* **37**, 025802 (2016).
- [19] M. Berry, *Czechoslovak Journal of Physics* **54**, 1039 (2004).
- [20] U. Günther, I. Rotter, and B. F. Samsonov, *J. Phys. A* **40**, 8815 (2007).
- [21] W. D. Heiss, *J. Phys. A* **45**, 444016 (2012).
- [22] I. Rotter, *J. Phys. A* **42**, 153001 (2009).
- [23] S. Garmon, I. Rotter, N. Hatano, and D. Segal, *Int. J. Theor. Phys.* **51**, 3536 (2012).
- [24] M. C. Toroker and U. Peskin, *J. Phys. B* **42**, 044013 (2009).
- [25] I. Rotter and J. P. Bird, *Rep. Prog. Phys.* **78**, 114001 (2015).
- [26] A. Delga, J. Feist, J. Bravo-Abad, and F. J. Garcia-Vidal, *Journal of Optics* **16**, 114018 (2014).
- [27] T. Gao, E. Estrecho, K. Y. Bliokh, T. C. H. Liew, M. D. Fraser, S. Brodbeck, M. Kamp, C. Schneider, S. Hofling, Y. Yamamoto, F. Nori, Y. S. Kivshar, A. G. Truscott, R. G. Dall, and E. A. Ostrovskaya, *Nature* **526**, 554 (2015).
- [28] M.-A. Miri and A. Alú, *Science* **363**, 42 (2019).
- [29] M. S. Ergoktas, S. Soleymani, N. Kakenov, K. Wang, T. B. Smith, G. Bakan, S. Balci, A. Principi, K. S. Novoselov, S. K. Ozdemir, and C. Kocabas, *Science* **376**, 184 (2022).
- [30] S. Soleymani, Q. Zhong, M. Mokim, S. Rotter, R. El-Ganainy, and Ş. K. Özdemir, *Nat. Commun.* **13**, 599 (2022).
- [31] D. Finkelstein-Shapiro, P.-A. Mante, S. Balci, D. Zigmantas, and T. Pullerits, “Non-Hermitian Hamiltonians for Linear and Nonlinear Optical Response: a Model for Plexitons,” (2022).
- [32] M. Brandstetter, M. Liertzer, C. Deutsch, P. Klang, J. Schöberl, H. E. Türeci, G. Strasser, K. Unterrainer, and S. Rotter, *Nat. Commun.* **5**, 4034 (2014).
- [33] A. Guo, G. J. Salamo, D. Duchesne, R. Morandotti, M. Volatier-Ravat, V. Aimez, G. A. Siviloglou, and D. N. Christodoulides, *Phys. Rev. Lett.* **103**, 093902 (2009).
- [34] C. Dembowski, B. Dietz, H.-D. Gräf, H. L. Harney, A. Heine, W. D. Heiss, and A. Richter, *Phys. Rev. Lett.* **90**, 034101 (2003).
- [35] B. Peng, c. K. Özdemir, M. Liertzer, W. Chen, J. Kramer, H. Yılmaz, J. Wiersig, S. Rotter, and L. Yang, *Proc. Natl. Acad. Sci.* **113**, 6845 (2016).
- [36] Y. Sun, W. Tan, H.-q. Li, J. Li, and H. Chen, *Phys. Rev. Lett.* **112**, 143903 (2014).
- [37] B. Peng, c. K. Özdemir, S. Rotter, H. Yilmaz, M. Liertzer, F. Monifi, C. M. Bender, F. Nori, and L. Yang, *Science* **346**, 328 (2014).
- [38] C. Dembowski, H.-D. Gräf, H. L. Harney, A. Heine, W. D. Heiss, H. Rehfeld, and A. Richter, *Phys. Rev. Lett.* **86**, 787 (2001).
- [39] S.-B. Lee, J. Yang, S. Moon, S.-Y. Lee, J.-B. Shim, S. W. Kim, J.-H. Lee, and K. An, *Phys. Rev. Lett.* **103**, 134101 (2009).
- [40] Y. Choi, S. Kang, S. Lim, W. Kim, J.-R. Kim, J.-H. Lee, and K. An, *Phys. Rev. Lett.* **104**, 153601 (2010).
- [41] H. Xu, D. Mason, L. Jiang, and J. G. E. Harris, *Nature* **537**, 80 (2016).
- [42] C. Jung, M. Müller, and I. Rotter, *Phys. Rev. E* **60**, 114 (1999).
- [43] H. Eleuch and I. Rotter, *Eur. Phys. J. D* **68**, 74 (2014).
- [44] W. D. Heiss, *Eur. Phys. J. D* **7**, 1 (1999).
- [45] C. Dembowski, B. Dietz, H.-D. Gräf, H. L. Harney, A. Heine, W. D. Heiss, and A. Richter, *Phys. Rev. E* **69**, 056216 (2004).
- [46] H. Haug and A.-P. Jauho, *Quantum Kinetics in Transport and Optics of Semiconductors*, second, substantially revised edition ed. (Springer, Berlin Heidelberg, 2008).
- [47] G. Stefanucci and R. van Leeuwen, *Nonequilibrium Many-Body Theory of Quantum Systems. A Modern Introduction*. (Cambridge University Press, 2013).
- [48] C. Yang, X. Wei, J. Sheng, and H. Wu, *Nat. Commun.* **11**, 4656 (2020).
- [49] M. Aspelmeyer, T. J. Kippenberg, and F. Marquardt, *Rev. Mod. Phys.* **86**, 1391 (2014).
- [50] F. Bemani, A. Motazedifard, R. Roknizadeh, M. H. Naderi, and D. Vitali, *Phys. Rev. A* **96**, 023805 (2017).
- [51] J. Sheng, X. Wei, C. Yang, and H. Wu, *Phys. Rev. Lett.* **124**, 053604 (2020).
- [52] D. R. Ward, D. A. Corley, J. M. Tour, and D. Natelson, *Nature Nanotechnol.* **6**, 33 (2011).
- [53] G. Baym and L. P. Kadanoff, *Phys. Rev.* **124**, 287 (1961).
- [54] G. Baym, *Phys. Rev.* **127**, 1391 (1962).
- [55] Y. Gao and M. Galperin, *J. Chem. Phys.* **144**, 174113 (2016).
- [56] S. Mukamel and M. Galperin, *J. Phys. Chem. C* **123**, 29015 (2019).
- [57] C. Caroli, R. Combescot, P. Nozieres, and D. Saint-James, *J. Phys. C: Solid State Phys.* **5**, 21 (1972).